IEEE Access
Multidisciplinary | Rapid Review | Open Access Journal

Received 10 January 2024, accepted 16 January 2024, date of publication 18 January 2024, date of current version 25 January 2024.

Digital Object Identifier 10.1109/ACCESS.2024.3355541

RESEARCH ARTICLE

Novel Powertrain Vibration Controller With Six Rules-Based Fuzzy Inference for Time-Fluctuated Control Period

HEISEI YONEZAWA, (Member, IEEE), ANSEI YONEZAWA, (Member, IEEE), AND ITSURO KAJIWARA

Division of Mechanical and Aerospace Engineering, Hokkaido University, Sapporo 060-8628, Japan

Corresponding author: Heisei Yonezawa (yonezawah@eng.hokudai.ac.jp)

This work was supported in part by the Japan Society for the Promotion of Science under Grants-in-Aid for Scientific Research Programs under Grant 22K20396 and Grant 23K13273, and in part by the Transmission Research Association for Mobility Innovation (TRAMI) under Grant 23B3-01.

ABSTRACT To ensure comfort and longevity of vehicle components, it is important to suppress low-frequency transient vibrations in the powertrain. This study proposes a unique technique for active vibration control that incorporates six rules-based fuzzy logic compensation. The technique addresses changes in control periods of an actuator over time. Firstly, a model prediction technique is used with a sampled-data controller (SDC) to address the highest possible phase delay in the control input caused by the fluctuating control period. In addition, fuzzy sets are utilized to define the changing renewal timings of the control input, which are distinct from the regular timings used by the periodically operated SDC. These fuzzy sets are named ''Nearly previous timing'' and ''Nearly upcoming timing''. This study employs six inference rules to achieve fuzzy compensation that resembles human intuition. These rules utilize output variables defined by linguistic fuzzy sets, such as ''Similar to commands from SDC'' and ''Very similar to commands from SDC'', making the inference process more flexible. Due to the utilization of the fuzzy sets and periodic control signals provided by the SDC, it is possible to reasonably deduce unknown control inputs at various update timings. To evaluate the effectiveness of the control scheme, simulations and experiments are conducted using an actual test setup to investigate its damping performance. The experimental findings indicate that the new active damping technique effectively minimizes transient powertrain vibrations. Furthermore, comparative studies with previous control systems indicate the improved performance and robustness of the proposed approach.

INDEX TERMS Fuzzy reasoning, restriction on control timing, sampled-data control, vehicle powertrain, vibration reduction.

I. INTRODUCTION

Vibrations produce noise, fatigue failure, and discomfort, all of which have a negative impact on mechanical systems. As a consequence of the present trend toward downsizing, more comfort, less weights, and better performance, there is a higher requirement for vibration suppression technologies [1], [2], [3], [4]. Active vibration damping has drawn a lot of study attention because it has the ability to provide powerful dampening effects for complex mechanical systems [5], [6].

Drivetrains of vehicles may undergo momentary vibrations when there are abrupt variations in torque or gear backlash. These oscillations have a negative impact on factors such as drivability, passenger comfort, and the lifespan of the vehicle. As a result, numerous studies have focused on finding ways to control these transient vibrations in powertrains. Many control strategies have been investigated, including sliding mode control [7], [8], switching control of linear-quadratic regulator (LQR) [9], and model reference adaptive Linear Quadratic

The associate editor coordinating the review of this manuscript and approving it for publication was Jesus Felez.

Tracking (ALQT) control [10]. Additionally, model predictive control (MPC) is widely used in many attempts [11], [12], [13], [14]. The complicated properties of powertrain systems, such as nonlinearities and mechanical constraints, are however accommodated by standard MPC through computationally intensive optimization calculations and elaborate modeling.

To implement active vibration control, an actuator must be utilized. Among the available options, engines have become a preferred choice because of their cost-effectiveness and high power output, serving as power sources for powertrains. Recently, there has been an increasing focus on the advancement of engines that operate with clean energy sources like hydrogen and biomass fuels [15]. This development aligns with the integration of these new engines into hybrid vehicles (HVs) that already exist, thereby generating significant interest in the field [16], [17]. As a result, active vibration control utilizing an engine [18] has become a significant area of focus.

However, the limitations on engine control periods create a more difficult situation for actively dampening powertrains. For instance, the control input, which is the engine torque, cannot be adjusted at regular intervals as shown in Fig. 1. The occurrence of updates is limited to a particular angle of rotation of the crankshaft, leading to the investigations of the following problems as the primary focus of this study.

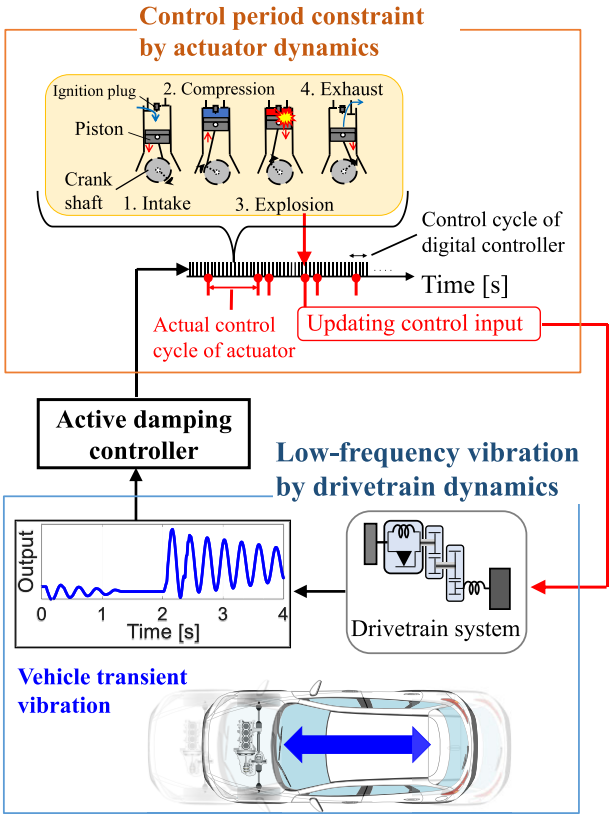

FIGURE 1. Constraint on the control cycle due to actuator dynamics.

Issue (a): First of all, while using digital vibration control, the discretization accuracy is degraded since the update intervals are much longer than the intended resonance frequency that needs suppression.

Issue (b): Furthermore, variances in vehicle speed contribute to differences in the time intervals of control for the actuator (i.e., time-fluctuated control period). This feature consequently induces the time-fluctuated timings of updates of the control input.

Earlier research has concentrated on examining the behavior and management of powertrain control systems, which include those powered by HV engines [18], [19], [20], [21], [22]. The use of real-time predictive controllers has shown potential in mitigating engine delay [18], [19]. Another effective strategy to combat the slow reaction of engines is to include an extra active damping actuator, i.e., a friction brake [20]. To deal with the changing dynamics over time, an adaptive disturbance observer-based harmonic rejection technique was used in another investigation [21].

Nevertheless, the conventional approaches mentioned earlier failed to address both issues (a) and (b) at the same time. In addition, there have been few attempts to prioritize simplicity in control systems and create a method that is understandable (reasonable) and has an easy-handling compensation mechanism. Although MPC-based approaches hold potential, accurately modeling complex powertrain characteristics within the limitations of the control period presents challenges in achieving a straightforward strategy.

Previously, we presented a vibration control system that confronted two problems: issues (a) and (b), which arise from the limitation on control period, to a certain extent [23]. To address discrete errors and the phase delay in the control input caused by variations in the control period, we employed a combination of a sampled-data H_2 controller and an MPC compensation mechanism in this system. Nevertheless, our prior method solely addressed the highest amount of phase lag in control inputs and failed to consider variations in the timing of updates, resulting in insufficient compensation for issue (b).

Fuzzy logic provides a quantitative approach to handle uncertainties, such as linguistic interpretations, through the utilization of membership functions and if-then logical inference rules. This effective technique allows for the representation of intricate systems. Notably, it excels in scenarios where accurate modeling of the system is challenging. For instance, it is employed in various intricate engineering problems [24] such as control system design [25], [26] including active powertrain vibration controllers [27].

To summarize the above, we give a brief overview of the existing approaches and why a novel control technique is needed. Although it is necessary to suppress low-frequency vibrations (primary resonance) in the powertrain for vehicle comfort and longevity, there are the two problems that hinder the high-performance vibration suppression, as indicated by issues (a) and (b) above. However, the existing approaches mentioned above cannot sufficiently address both issues (a)

and (b) at the same time. Therefore, a novel control strategy is needed to tackle the two issues by a straightforward and easy-handling compensation mechanism.

The objective of this study is to develop a drivetrain active damping controller that can deal with the above issues (a) and (b) simultaneously. As a goal of this objective, the effectiveness as well as the robustness of the proposed controller to the time-fluctuated control periods needs to be demonstrated in simulation and experimental verifications.

This paper introduces an innovative approach to actively control vibrations in the drivetrain of a vehicle by considering variable timings for updating control inputs. We use a sampled-data H_2 controller along with fuzzy logic to overcome the problem of irregular intervals for updating inputs. Issue (a) (i.e., effects of controller's discretized errors) is dealt with by the sampled-data H_2 controller [23], while issue (b) (i.e., variations in the update timing) is dealt with via fuzzy logic. This strategy revolves around utilizing fuzzy logic to handle situations where the timing of input updates deviates from the fixed periodic controller. The approach involves representing the update timings using fuzzy sets such as "Nearly previous timing," "Nearly upcoming timing," and "Nearly intermediate timing." By combining control signals from the fixed periodic controller, the fuzzy sets, and fuzzy rules designed to imitate human intuition, we determine control inputs at uncertain fluctuating times. Although the basis of such fuzzy compensation has been established in our studies [27], [28], the previous approach has only four inference rules composed of two fuzzy output variables. Due to its lack of flexibilities (flexible inferences) with abundant linguistic expressions, it may result in deteriorations of the robustness. To improve the robustness, this study presents a new compensation strategy based on six fuzzy rules including abundant linguistic output variables, leading to a rich diversity of control commands.

The principal contribution of this study is to propose a novel drivetrain vibration controller that addresses the issue (a) by the application of SDC while handling the issue (b) by a six rules-based fuzzy compensation approach. The paper's three unique contributions can be more detailed as follows:

(C1). Compared to the existing works [18], [23], the new contribution of this paper is to address the actuator's variable timings in updating control input (issue (b)) by developing a six rules-based fuzzy compensation approach. This approach simplifies the compensation mechanism by emulating qualitative decisions resembling human thinking. Another advantage is that the fuzzy compensation eliminates the need for intricate and detailed modeling of control input update timings.

(C2). In order to overcome the issue of discretization errors (issue (a)) that are increased for a digital controller due to an extended control period, this study introduces a sampled data controller (referred to as SDC).

(C3). In contrast to a prior study that only demonstrated simulation data and lacked essential experimental tests [28], this article confirms the proposed approach through simulations and experiments utilizing a physical test device. The experimental setup involves a simplified version of a real vehicle drivetrain. The simulations and experiments confirm the robustness of the proposed approach in dealing with substantial time-changes in the control period.

II. EXPERIMENTAL SYSTEM

A. EXPERIMENTAL DEVICE

A basic experimental device, whose specifications can be found in Table 1, is employed as the controlled plant.

To examine the fundamental aspects of vibration occurrences resulting from sudden shifts in the propelling force and the impacts of backlash, a simplified configuration is employed to replicate a real drivetrain [29], [30], [31] (see Fig. 2). This configuration emulates a

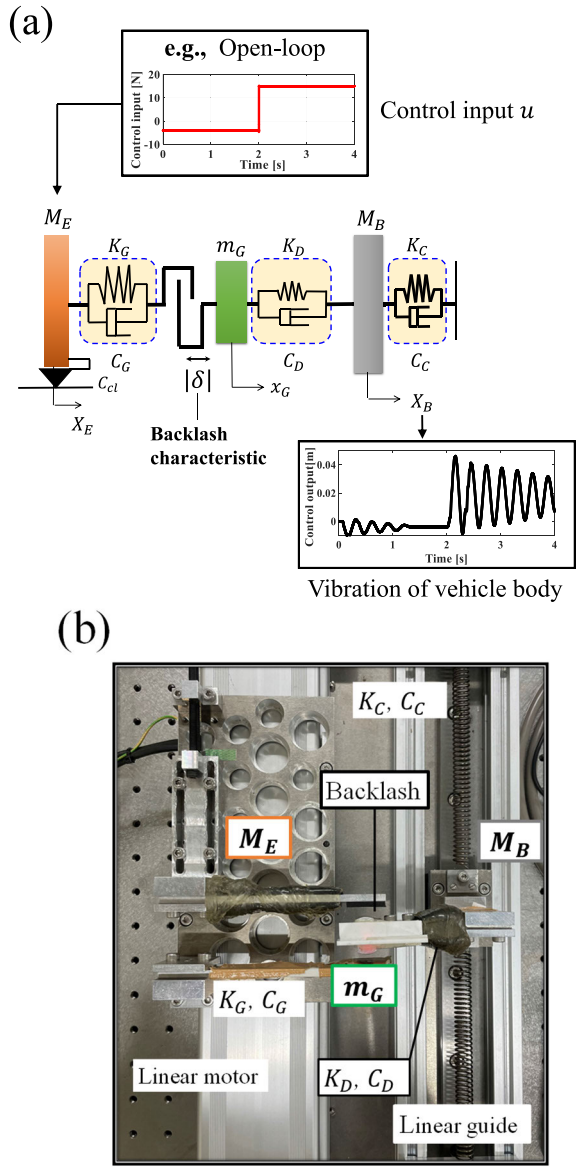

FIGURE 2. Abstract drivetrain mechanism: (a) dynamical model and (b) experimental apparatus.

TABLE 1. Parameters of drivetrain model.

Parameter	Value	Unit
M_B	0.232	kg
m_G	0.039	kg
M_E	1.04	kg
K_C	660.0	N/m
K_D	1.5×10^4	N/m
K_G	2.7×10^4	N/m
C_C	0.3	Ns/m
C_D	7.5	Ns/m
C_G	29.0	Ns/m
C_{cl}	4.0	Ns/m

three-degrees-of-freedom oscillation model comprising mass points (M_E, m_G, and M_B). To represent backlash, a dead-zone band is introduced, delimited by leaf springs on both sides of m_G. More information on the test instrument can be found elsewhere [29], [30], [31]. The actuator is constituted by the motor and the control period limitation, which will be discussed later.

B. MODEL

The experimental device contains backlash and other non-linearities. However, a linearized model is necessary for the construction of the base vibration controller. The time varying linear state equation of the plant is given as [23], [29], and [30], see (1)–(4), as shown at the bottom of the page, where $\boldsymbol{w}_p$ stands for the disturbance, which includes the effect of backlash, and u stands for the control input. The dead-zone feature of backlash is formulated via switching on the parameter Sw. This formulation has been provided by [32] and [33]

$$F = Sw \cdot K_G \cdot (X_E - x_G) + OKG$$

$$Sw = \begin{cases} 1, & X_E - x_G > |\delta| \\ 1, & X_E - x_G < -|\delta| \\ 0, & |X_E - x_G| \le |\delta| \end{cases},$$

$$OKG = \begin{cases} -|K_G \times |\delta||, & X_E - x_G > |\delta| \\ |K_G \times |\delta||, & X_E - x_G < -|\delta| \\ 0, & |X_E - x_G| \le |\delta| \end{cases} \quad (5)$$

where, in the SDC design, $|\delta|$ and F, respectively, stand for the width of the dead zone and the force of the rigidity K_G. Sw in this design has a value of 1.0.

III. ACTUATOR'S LONG PERIOD OF CONTROL WITH TIME VARIATIONS

A. CONSTRAINT ON CONTROL PERIOD

The experimental setup shown in Fig. 2(b) contains a motor functioning as the actuator. We focus on the essential aspect related to the limitation of control period, in principle, equivalent to that of a real engine, in order to examine issues (a) and (b) on the control period. The digital signal processor (DSP) employs software to enforce this limitation for the motor. In this study, issues (a) and (b) are owing to the control period restriction, which is incorporated into the software of the experimental system. The overall closed-loop experimental setup is depicted in Fig. 3(a). The timing for updating the actual control inputs is limited (fluctuated) due to longer and time-varying control periods specified by the aforementioned software, despite the capability of a control system in the DSP to calculate control input commands for vibration control at shorter and consistent intervals.

Fig. 3(b) illustrates the patterns of time-fluctuated control periods. The studies examined two instances of fluctuation, referred to as Cases 1 and 2, which are similar to the ones shown in Fig. 3(b). Depending on these fluctuating control intervals, the DSP maintains a consistent value for the actual control input applied to the motor. In Case 1 of Fig. 3(b), the frequency at which the actuator's control input is updated varies between 2.0 and 4.0 s, occurring approximately 5 to 9 times the vehicle's resonance frequency of 4 Hz, which is the desired frequency to be attenuated.

$$\dot{\boldsymbol{x}}_p = \boldsymbol{A}_p \boldsymbol{x}_p + \boldsymbol{B}_{p1} \boldsymbol{w}_p + \boldsymbol{B}_{p2} u \quad (1)$$

$$y_p = \boldsymbol{C}_p \boldsymbol{x}_p + \boldsymbol{D}_{p1} \boldsymbol{w}_p + D_{p2} u \quad (2)$$

$$\boldsymbol{A}_p = \begin{bmatrix} 0 & 0 & 0 & 1 & 0 & 0 \\ 0 & 0 & 0 & 0 & 1 & 0 \\ 0 & 0 & 0 & 0 & 0 & 1 \\ -\frac{(K_D+K_C)}{M_B} & \frac{K_D}{M_B} & 0 & -\frac{(C_D+C_C)}{M_B} & \frac{C_D}{M_B} & 0 \\ \frac{K_D}{m_G} & -\frac{(SwK_G+K_D)}{m_G} & \frac{SwK_G}{m_G} & \frac{C_D}{m_G} & -\frac{(SwC_G+C_D)}{m_G} & \frac{SwC_G}{m_G} \\ 0 & \frac{SwK_G}{M_E} & -\frac{SwK_G}{M_E} & 0 & \frac{SwC_G}{M_E} & -\frac{(SwC_G+C_{cl})}{M_E} \end{bmatrix}$$

$$\boldsymbol{B}_{p1} = \begin{bmatrix} 0 & 0 & 0 & 0 & \frac{1}{m_G} & -\frac{1}{M_E} \\ 0 & 0 & 0 & \frac{1}{M_B} & 0 & 0 \end{bmatrix}^T, \boldsymbol{B}_{p2} = \begin{bmatrix} 0 & 0 & 0 & 0 & 0 & \frac{1}{M_E} \end{bmatrix}^T, \boldsymbol{C}_p = \begin{bmatrix} 1 & 0 & 0 & 0 & 0 & 0 \end{bmatrix}$$

$$\boldsymbol{D}_{p1} = 0, D_{p2} = 0 \quad (3)$$

$$\boldsymbol{x}_p = \begin{bmatrix} X_B & x_G & X_E & \dot{X}_B & \dot{x}_G & \dot{X}_E \end{bmatrix}^T \quad (4)$$

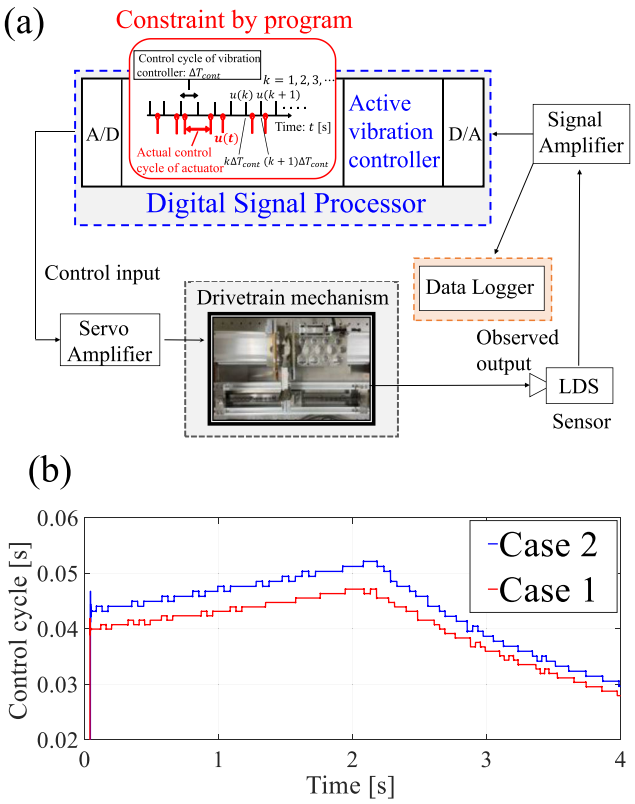

FIGURE 3. The experimental setup: (a) a closed-loop configuration, and (b) two instances where the control cycle is fluctuated.

B. TIMING VARIATIONS FOR UPDATES

Fig. 4 depicts a graphical representation of the control input command acquired from a controller (illustrated as a solid black line) and the corresponding real input provided by the actuator (displayed as a dashed red line). Figure 4 clearly illustrates the main problem this work seeks to address.

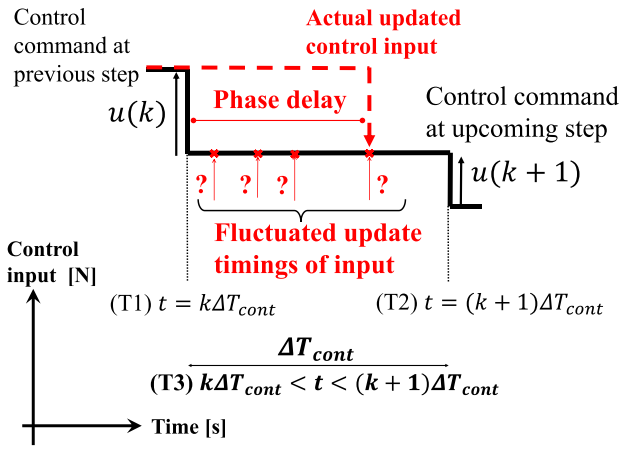

FIGURE 4. Varying timings of control input updates compared to those of a fixed periodic SDC.

The actuator and the fixed periodic controller, which runs at a period of ΔT_{cont}, have different update timings since the control period fluctuates. The timing error leads to a phase lag in the control input, which diminishes the efficiency of vibration control.

The purpose of this research is to establish the suitable control instructions for the actuator during the time interval (T3), with the condition that $k\Delta T_{cont} < t < (k+1)\Delta T_{cont}$, based on the given periodic control command values $u(k)$ at (T1) $t = k\Delta T_{cont}$ and $u(k+1)$ at (T2) $t = (k+1)\Delta T_{cont}$.

IV. PROPOSED METHOD FOR MITIGATING VIBRATIONS THROUGH ACTIVE DAMPING

A. ALGORITHM FOR MODEL PREDICTION UTILIZING SDC

The proposed method is comprised of two components, as demonstrated in Fig. 5. It involves utilizing the SDC [23] for a model predictive algorithm, along with incorporating straightforward fuzzy logic compensation to consider the variances in the timing of control input updates.

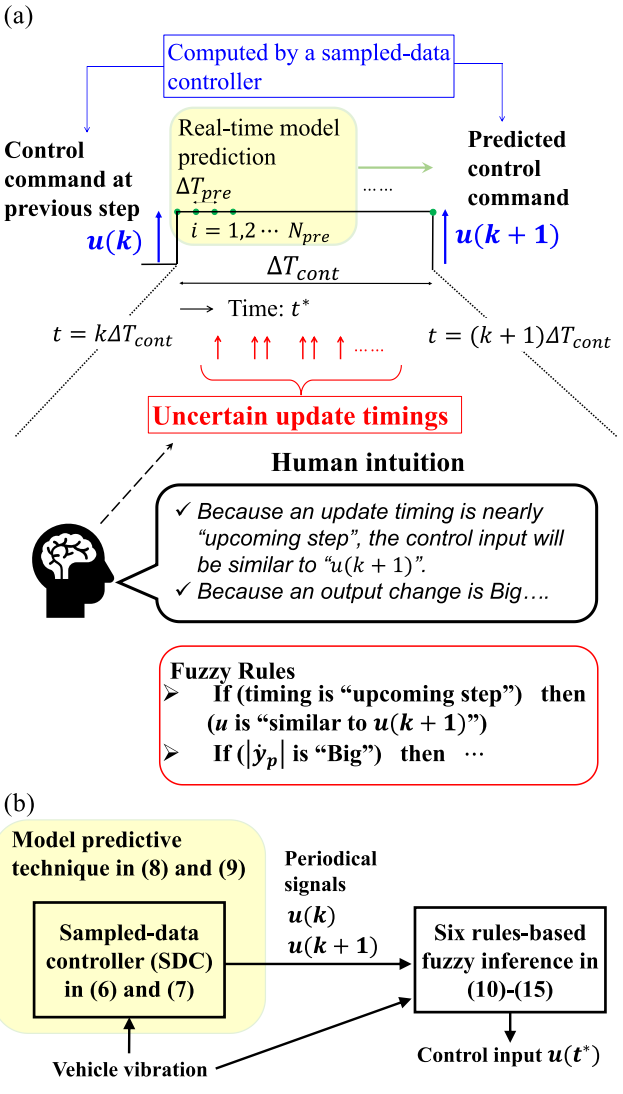

FIGURE 5. The vibration control approach presented in this study: (a) overall control system, and (b) relationship between the fuzzy inference part and SDC in the model predictive part.

Employing digital controllers under an extension of the update intervals for the input leads to highlighting discretization error issues. The control performance of a digital vibration controller degrades as the actuator control period is extended, according to earlier studies [23], [30]. However, the use of a sampled data controller (SDC) can circumvent this problem [34], [35]. The SDC can be designed and implemented in a way that avoids discretization. Hence, we employ a fixed periodic sampled data H_2 controller [34], [35] in this scenario with a calculation period denoted as ΔT_{cont}, owing to its simplicity and ease of implementation.

The digital control form for the sampled data H_2 controller is directly derived from the continuous-time plant mentioned in Eqs. (1)–(4). Therefore, there is no need for discrete approximations in the implementation process. There are more details on the controller design [23]. The resulting controller is expressed as a discrete-time state equation,

$$\boldsymbol{x}_c(k+1) = \boldsymbol{A}_c\boldsymbol{x}_c(k) + \boldsymbol{B}_c\left(X_B(k\Delta T_{cont}) - r(k\Delta T_{cont})\right) \tag{6}$$

$$u(k) = \boldsymbol{C}_c\boldsymbol{x}_c(k) + D_c\left(X_B(k\Delta T_{cont}) - r(k\Delta T_{cont})\right) \tag{7}$$

where the target signal, denoted as $r(k\Delta T_{cont})$, represents a smooth step reference without any oscillations when there is a sudden change in the propelling force of a real vehicle. The state variable in the SDC is $\boldsymbol{x}_c(k)$, where k indicates the number of computation steps at ΔT_{cont} (i.e., SDC's periodical steps). The measured output, $y_p = X_B$, corresponds to the vibration of the body of the vehicle. At step $t = k\Delta T_{cont}$, the control command $u(k)$ is determined by combining Eqs. (6) and (7), along with the feedforward input of the reference signal [29], [30].

Next, the control period, which changes over time, causes phase delays in the control input that drives the actuator. These delays are illustrated in Fig. 4 and contribute to the amplification of vibrations in the vehicle body. In this context, only the largest phase delay, ΔT_{cont}, is considered. The future (upcoming) control signal $u(k+1)$ from the SDC at step $t = (k+1)\Delta T_{cont}$ must be acquired at step $t = k\Delta T_{cont}$ in order to perform phase-delay compensation for the maximal delay ΔT_{cont}. To achieve this, a model predictive technique, which utilizes the SDC and a time-varying linear Kalman filter, is implemented [23]. From the viewpoint of the overall control system shown in Fig. 5 (a), the contribution of the model predictive technique with the SDC is to provide periodical control signals $u(k), u(k+1)\cdots$. Then, the periodical control signals $u(k)$ and $u(k+1)$ are delivered to the fuzzy inference part to compute control signals $u(t^*)$ at fluctuating update timings. The predicted value of $u(k+1)$, which should be known at $t = k\Delta T_{cont}$, is required for performing the fuzzy inference compensation explained in the next section. Using the time-varying state equation of the plant model, this approach carries out iterative-simulation-based prediction with a small period $\Delta T_{predict}$. Then, operating the SDC in (6) and (7) results in the delivery of $u(k+1)$ of the next step $t = (k+1)\Delta T_{cont}$. This predictive simulation occurs at step $t = k\Delta T_{cont}$ (see Fig. 5). Therefore, the model predictive algorithm is composed of estimation of an initial condition by the Kalman filter, online simulation of the plant dynamics, and execution of the SDC to derive $u(k+1)$. This algorithm can be implemented with a for-loop from $i = 1$ to $N_{pre} = (\Delta T_{cont}/\Delta T_{predict}) + 1$. i is loop counter, and N_{pre} is the maximum number of iterations for the model prediction. Specifically, during the time interval from (T1) $t = k\Delta T_{cont}$ to (T2) $t = (k+1)\Delta T_{cont}$, with N_{pre} steps, the plant is simulated in real-time as

$$\begin{aligned}\boldsymbol{x}_{pd}[i+1] &= \boldsymbol{A}_{pd}\boldsymbol{x}_{pd}[i] + \boldsymbol{B}_{p1d}\boldsymbol{w}_p[i] + \boldsymbol{B}_{p2d}u[i] \\ &= \left\{\boldsymbol{I}_{6\times 6} + \Delta T_{predict}\cdot\boldsymbol{A}_p(t)\right\}\boldsymbol{x}_{pd}[i] \\ &\quad + \left\{\Delta T_{predict}\cdot\boldsymbol{B}_{p1}(t)\right\}\boldsymbol{w}_p[i] \\ &\quad + \{\Delta T_{predict}\cdot\boldsymbol{B}_{p2}(t)\}u[i] \end{aligned} \tag{8}$$

$$\begin{aligned} y_{pd}[i] &= \boldsymbol{C}_{pd}\boldsymbol{x}_{pd}[i] + \boldsymbol{D}_{p1d}\boldsymbol{w}_p[i] + D_{p2d}u[i] \\ &= \boldsymbol{C}_p(t)\,\boldsymbol{x}_{pd}[i] \end{aligned} \tag{9}$$

where $i = 1, 2, \cdots N_{pre}$ and $N_{pre} = (\Delta T_{cont}/\Delta T_{predict}) + 1$. Based on the time-varying switched linear state equation of the experimental apparatus, which includes nonlinearities such as backlash, the online calculations are performed for the discrete-time systems (8) and (9) [29], [30]. The control input used to operate the actuator is denoted as $u[i]$, while the external input taking backlash into consideration is represented by $\boldsymbol{w}_p[i]$.

Initial conditions are necessary for the simulation. The time-varying switched linear state equation and Kalman filtering theory are utilized to estimate the value of the state variable $\boldsymbol{x}_{pd}[i]$ [23], [31].

The SDC ($\boldsymbol{A}_c$, $\boldsymbol{B}_c$, $\boldsymbol{C}_c$, $\boldsymbol{D}_c$) is represented in state-space form, and it generates the output $u(k+1)$ at the next computation instant $t = (k+1)\Delta T_{cont}$, with ΔT_{cont} being the computation period. As a result, by employing the SDC incorporated within the real-time simulation, the value of $u(k+1)$ can be estimated at the time step $t = k\Delta T_{cont}$.

The six rules-based fuzzy inference is combined with the SDC and model prediction part by delivering the periodical control signals $u(k)$ and $u(k+1)$, which are outputted from the SDC in the model prediction part, to the fuzzy inference part. In other words, the fuzzy inference part and the SDC are connected in series via the transmission of $u(k)$ and $u(k+1)$. The relationship between the two (i.e., how the fuzzy inference is combined with the SDC) is illustrated in Fig. 5(b). Based on $u(k)$ and $u(k+1)$ given from the SDC and the model prediction, the six fuzzy rules execute inference to compute control signals $u(t^*)$ at fluctuating update timings.

In summary, the step-by-step process of the model prediction technique is indicated below.

(Process 1): The time-varying linear Kalman filter estimates the state variable $\boldsymbol{x}_{pd}[i=1]$. Then, $\boldsymbol{x}_{pd}[i=1]$ is delivered to the model prediction part as the initial condition.

(Process 2): At $t = k\Delta T_{cont}$, the plant model is simulated in real-time from (T1) $t = k\Delta T_{cont}$ to

(T2) $t = (k+1)\Delta T_{cont}$. Specifically, the state-space representation (8) and (9) is iteratively operated with $i = 1, 2, \cdots N_{pre}$ and $N_{pre} = (\Delta T_{cont}/\Delta T_{predict})+1$. As a result, we can obtain the output $y_{pd}\left[N_{pre}\right]$.

(Process 3): According to $y_{pd}\left[N_{pre}\right]$ and r, the SDC (6) and (7) is operated to compute $u(k+1)$. This operation is executed at $t = (k+1)\Delta T_{cont}$ within the real-time simulation (i.e., $i = N_{pre}$ within a for-loop).

(Process 4): $u(k)$ and $u(k+1)$, which have been outputted from the SDC, are then delivered to the six rules-based fuzzy inference part, as shown in Fig. 5(b). Based on $u(k)$ and $u(k+1)$ given from the SDC, the six fuzzy rules execute inference to compute control signals $u(t^*)$ at fluctuating update timings.

B. SIX RULES-BASED FUZZY INFERENCE EMPLOYED TO ADDRESS THE ISSUE OF COMPENSATING FOR DIFFERENCES IN THE TIMING OF CONTROL INPUT UPDATES

A straightforward method of fuzzy inference compensation is introduced to determine the control input values that are updated at varying timings between $t = k\Delta T_{cont}$ and $t = (k+1)\Delta T_{cont}$ (i.e., $k\Delta T_{cont} < t < (k+1)\Delta T_{cont}$). The concept of the fuzzy strategy is shown in Fig. 5.

If the update timing of the actuator aligns perfectly with either $t = k\Delta T_{cont}$ or $t = (k+1)\Delta T_{cont}$, it is logically acceptable to refer to $u(k)$ or $u(k+1)$ as the control input, respectively. However, when the timing of the control input update varies, it deviates from the periodic sampled-data H_2 controller's timing within the range of $k\Delta T_{cont} < t < (k+1)\Delta T_{cont}$. In such cases, the following inference issue, which is based on known information (e.g., if $t = (k+1)\Delta T_{cont}$ then $u(t) = u(k+1)$), needs to be considered to derive the control inputs updated at uncertain timings.

The proposed approach is based on the concept that changes in the timing of control input updates can be represented by fuzziness. The predetermined periodic computation timings: the future (i.e., upcoming) step ($t = (k+1)\Delta T_{cont}$) and the past (i.e., previous) step ($t = k\Delta T_{cont}$) of the sampled-data controller are linked with fuzziness. Specifically, fuzzy sets such as: "**Nearly** previous step $t = k\Delta T_{cont}$", "**Nearly** intermediate step $t = (k+1/2)\Delta T_{cont}$ before it", "**Nearly** intermediate step $t = (k+1/2)\Delta T_{cont}$ after it", and "**Nearly** upcoming step $t = (k+1)\Delta T_{cont}$" are defined to address control input update timing that deviates from that of a fixed periodic controller. To handle the fluctuating update timing, the degree of proximity (closeness) to these four update timings is evaluated within the range of $k\Delta T_{cont} < t < (k+1)\Delta T_{cont}$. Additionally, fuzziness on control inputs is also employed to incorporate qualitative and intuitive (i.e., human-thought-like) knowledge that suggests

(Knowledge 1): *An unknown control input updated close to* $t = k\Delta T_{cont}(t = (k+1)\Delta T_{cont})$ *should be similar to* $u(k)$ $(u(k+1))$.

That is, fuzziness is linked to the control commands $u(k)$ at the previous step and $u(k+1)$ at the upcoming step. The two commands are computed in Section IVA.

A suitable control input can be determined by combining fuzzy sets with periodic control signals from SDC and accurately analyzing the factor of how closely the fluctuating update timing aligns with the predetermined steps. Compared to the previous fuzzy inference [27], [28], this study introduces four fuzzy sets: "Similar to $u(k)$", "Similar to $u(k+1)$", "Very similar to $u(k)$", and "Very similar to $u(k+1)$". These linguistic fuzzy output variables are aimed at providing more various candidates of the resultant control commands by the fuzzy compensation.

Our fuzzy rules also evaluate the rate of change with time in the control output. Specifically, we evaluate the absolute value of the vibration in the vehicle body velocity, denoted as $\dot{y}_p = \dot{X}_B$, for the drivetrain in Eqs. (1) and (2). The inference rules are based on the following intuitive concept:

(Knowledge 2): *If the fluctuation of the control output increases in the future, the impact of the phase delay in the control input will become more severe. Hence, when the update timing occurs during the latter half of the control period, the predicted control input provides improved compensation for the phase delay.*

As a result, this study offers the enhanced fuzzy compensation made up of the six rules illustrated below. These six rules are based on the abundant linguistic expressions of the output variables. They are combinations of the fuzziness such as "Similar to…" or "Very similar to…" and the periodic optimal commands "$u(k)$, $u(k+1)$, $u(k+2)$…" from SDC. The proposed six rules-based inference offers a higher level of adaptability and flexibility in managing fluctuations in the timing of control input updates.

(Rule 1):

$$\begin{aligned}&\text{IF } (t^* \text{ is nearly upcoming step } (\Delta T_{cont}))\\ &\quad\text{THEN } (u(t^*) \text{ is similar to } u(k+1))\end{aligned} \tag{10}$$

(Rule 2):

$$\begin{aligned}&\text{IF } (t^* \text{ is nearly previous step } (0))\\ &\quad\text{THEN } (u(t^*) \text{ is similar to } u(k))\end{aligned} \tag{11}$$

(Rule 3):

$$\begin{aligned}&\text{IF } (t^* \text{ is nearly intermediate step } (\frac{1}{2}\Delta T_{cont}) \text{ after it})\\ &\quad\text{and } (\left|\dot{y}_p\right| \text{ is Big})\\ &\quad\text{THEN } (u(t^*) \text{ is very similar to } u(k+1))\end{aligned} \tag{12}$$

(Rule 4):

$$\begin{aligned}&\text{IF } (t^* \text{ is nearly intermediate step } (\frac{1}{2}\Delta T_{cont}) \text{ after it})\\ &\quad\text{and } (\left|\dot{y}_p\right| \text{ is Small})\\ &\quad\text{THEN } (u(t^*) \text{ is similar to } u(k+1))\end{aligned} \tag{13}$$

(Rule 5):

$$\begin{aligned}&\text{IF } (t^* \text{ is nearly intermediate step } (\frac{1}{2}\Delta T_{cont}) \text{ before it})\\ &\quad\text{and } (\left|\dot{y}_p\right| \text{ is Big})\\ &\quad\text{THEN } (u(t^*) \text{ is similar to } u(k))\end{aligned} \tag{14}$$

(Rule 6):

IF (t^* is nearly intermediate step ($\frac{1}{2}\Delta T_{cont}$) before it)
and ($|\dot{y}_p|$ is Small)
THEN ($u(t^*)$ is very similar to $u(k)$) (15)

where the input variable, t^*, is specified as $t^* = t - k\Delta T_{cont}$ within the range of $0 < t^* < \Delta T_{cont}$ with regard to time t ($k\Delta T_{cont} < t < (k+1)\Delta T_{cont}$). The control input at that moment (t^*) is represented by the output variable $u(t^*)$. Due to its simplicity, Tsukamoto-type fuzzy inference [36], [37] is used in this case for Rules 1–6.

(Rule 1) is operated to apply the above-mentioned (Knowledge 1) for $u(k+1)$ already calculated at $t = (k+1)\Delta T_{cont}$. Concretely, the intuitive knowledge, "*The closer a control input update timing is to* $t = (k+1)\Delta T_{cont}$, *the more similar its proper value should be to* $u(k+1)$", is translated into (Rule 1). In the same manner, the role of (Rule 2) is to apply (Knowledge 1) for $u(k)$ calculated at $t = k\Delta T_{cont}$. During the latter half of the control period, (Rule 3) and (Rule 4) consider the above-mentioned (Knowledge 2). They help the inference process judge how much the utility of the phase delay compensation needs to be introduced. In their operations, this decision depends on not only timings but also the rate of change in the control output. In particular, the priority is focused on $u(k+1)$ because (Rule 3) and (Rule 4) use (Knowledge 2) in the latter half of the control period. In (Rule 3), the effect of $u(k+1)$ is reflected more intensely in the output by using the linguistic expression "Very similar to $u(k+1)$". In the same way, (Rule 5) and (Rule 6) are operated to consider (Knowledge 2) during the first half of the control period.

The operation of these rules is based on the combination of (Knowledge 1) and (Knowledge 2), i.e., a blend of Rules 1, 2, 3, 4, 5, and 6., resulting in reasonable control signals.

For the input variable t^*, the fuzzy sets "nearly upcoming step (ΔT_{cont})", "nearly previous step (0)", "nearly intermediate step ($1/2\Delta T_{cont}$) after it", and "nearly intermediate step ($1/2\Delta T_{cont}$) before it" are defined as triangular membership functions $h^t_{upcoming}$, $h^t_{previous}$, and $h^t_{middlea}$, and $h^t_{middleb}$ respectively. "Big" and "Small" are represented by the functions h^{cy}_{Big} and h^{cy}_{Small}, respectively, for the input variable $|\dot{y}_p|$,.

$$h^t_{upcoming} = \frac{1}{\Delta T_{cont}} \cdot t^* \tag{16}$$

$$h^t_{previous} = -\frac{1}{\Delta T_{cont}} \cdot t^* + 1 \tag{17}$$

$$h^t_{middlea} = \begin{cases} \dfrac{2}{\Delta T_{cont}} \left(-\left(t^* - \dfrac{1}{2}\Delta T_{cont} \right) + \dfrac{1}{2}\Delta T_{cont} \right), \\ \qquad t^* \geq \Delta T_{cont}/2 \\ 0, \\ \qquad t^* < \Delta T_{cont}/2 \end{cases} \tag{18}$$

$$h^t_{middleb} = \begin{cases} \dfrac{2}{\Delta T_{cont}} \cdot t^*, & t^* \leq \Delta T_{cont}/2 \\ 0, & t^* > \Delta T_{cont}/2 \end{cases} \tag{19}$$

$$h^{cy}_{Big} = \frac{1}{|\dot{y}_p|_{max}} \cdot |\dot{y}_p| \tag{20}$$

$$h^{cy}_{Small} = -\frac{1}{|\dot{y}_p|_{max}} \cdot |\dot{y}_p| + 1 \tag{21}$$

The maximum value within the range of $|\dot{y}_p|$ is shown by $|\dot{y}_p|_{max}$. A membership degree of 0 or 1 corresponds to values above $|\dot{y}_p|_{max}$. In other words, the tuning parameter for h^{cy}_{Small} and h^{cy}_{Big} is $|\dot{y}_p|_{max}$. The membership functions with regards to t^* and $|\dot{y}_p|$ are described in Fig. 6 (a) and (b), respectively. Because the magnitude of each membership function is limited within the range from 0 to 1 at all points, all of them used in the proposed fuzzy system have the proper forms. This study employs Tsukamoto-type fuzzy inference [36], [37]. According to this type, right-angled triangular membership functions are required as shown in Fig. 6(a). In addition, an input variable to the fuzzy system of this study is an update timing t^* of the control input. Therefore, the membership functions require shapes and conditions, which are different from those used in conventional fuzzy PID controllers by Mamdani-method.

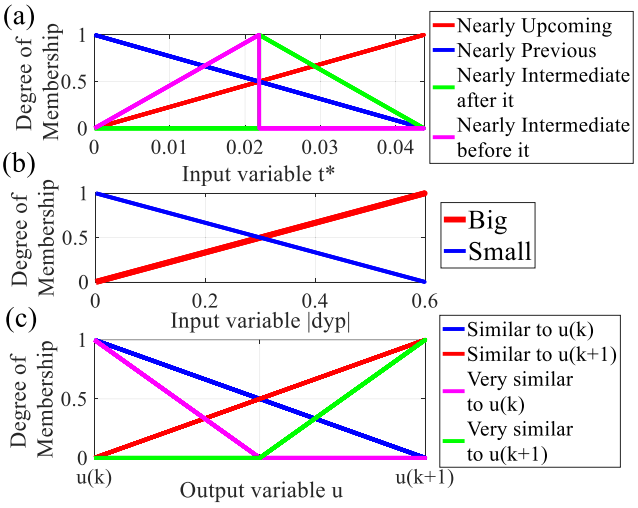

FIGURE 6. Examples of the membership functions used in this study.

Given the current condition, the rule's antecedent part calculates the degree of match w_i ($0 \leq w_i \leq 1, i = 1, 2, \ldots 6$) for Rules 1–6 as follows.

$$w_1 = h^t_{upcoming}(t^*) \tag{22}$$

$$w_2 = h^t_{previous}(t^*) \tag{23}$$

$$w_3 = h^t_{middlea}(t^*) \times h^{cy}_{Big}(|\dot{y}_p|) \tag{24}$$

$$w_4 = h^t_{middlea}(t^*) \times h^{cy}_{Small}(|\dot{y}_p|) \tag{25}$$

$$w_5 = h^t_{middleb}(t^*) \times h^{cy}_{Big}(|\dot{y}_p|) \tag{26}$$

$$w_6 = h^t_{middleb}(t^*) \times h^{cy}_{Small}(|\dot{y}_p|) \tag{27}$$

Next, the fuzzy rule's output is determined by reflecting the degree of match $w_1, w_2 \ldots w_6$ on the rule's consequent. How to define linguistic fuzzy sets, like "Similar to commands from SDC" and "Very similar to commands from SDC," is as follows. For the control commands $u(k)$ and $u(k+1)$ from SDC, it is firstly needed to consider membership functions with the horizontal axis as the control input candidates and the vertical axis as the membership degree (degree of match) from 0 to 1, as shown in Fig. 6(c). Then, the linguistic fuzzy sets can be defined by constructing the membership functions according to Eqs. (28)-(31) in real time based on the use of $u(k)$ and $u(k+1)$. This process means that fuzziness is added to $u(k)$ and $u(k+1)$ by giving membership degrees to control input values other than $u(k)$ and $u(k+1)$ in the set of control input candidates on the horizontal axis. In Eqs. (28)-(31), the membership functions: $h^u_{upcoming}$, $h^u_{previous}$, h^u_{veryup}, $h^u_{verypre}$, respectively, are used to define the four fuzzy sets: "similar to $u(k+1)$", "similar to $u(k)$", "very similar to $u(k+1)$", and "very similar to $u(k)$". These membership functions are described in Fig. 6(c). Right-angled triangular monotonic membership functions are used in Tsukamoto-type fuzzy inference [36], [37] as

$$h^u_{upcoming} = \begin{cases} \dfrac{1}{\Delta u}\left(u - u\left(k\right)\right) & \text{if } u(k) < u(k+1) \\ -\dfrac{1}{\Delta u}\left(u - u\left(k+1\right)\right) + 1 & \text{if } u(k+1) < u(k) \end{cases} \tag{28}$$

$$h^u_{previous} = \begin{cases} -\dfrac{1}{\Delta u}\left(u - u\left(k\right)\right) + 1 & \text{if } u(k) < u(k+1) \\ \dfrac{1}{\Delta u}\left(u - u\left(k+1\right)\right) & \text{if } u(k+1) < u(k) \end{cases} \tag{29}$$

$$h^u_{veryup} = \begin{cases} \dfrac{2}{\Delta u}\left(u - \left(u\left(k\right) + \dfrac{\Delta u}{2}\right)\right) & \text{if } u(k) < u(k+1) \\ -\dfrac{2}{\Delta u}\left(u - u\left(k+1\right)\right) + 1 & \text{if } u(k+1) < u(k) \end{cases} \tag{30}$$

$$h^u_{verypre} = \begin{cases} -\dfrac{2}{\Delta u}\left(u - u\left(k\right)\right) + 1 & \text{if } u(k) < u(k+1) \\ \dfrac{2}{\Delta u}\left(u - \left(u\left(k+1\right) + \dfrac{\Delta u}{2}\right)\right) & \text{if } u(k+1) < u(k) \end{cases} \tag{31}$$

where $\Delta u = |u(k+1) - u(k)|$.

Note that Fig. 6 (c) shows the just numerical examples because $h^u_{upcoming}$, $h^u_{previous}$, h^u_{veryup}, and $h^u_{verypre}$ are automatically constructed using $u(k)$ and $u(k+1)$ changing in real time. The inference result u_i $(i = 1, 2, \ldots 6)$ in each rule can be determined using fuzzy reasoning of the Tsukamoto type by substituting $w_1, w_2 \ldots w_6$ for the inverse function of $h^u_{upcoming}(u)$, $h^u_{previous}(u)$, $h^u_{veryup}(u)$, or $h^u_{verypre}(u)$, which is represented by as

(Case 1): $u(k) < u(k+1)$

$$u_1 = {h^u_{upcoming}}^{-1}(w_1) = u(k) + w_1 \Delta u \tag{32}$$
$$u_2 = {h^u_{previous}}^{-1}(w_2) = u(k) - (w_2 - 1)\,\Delta u \tag{33}$$
$$u_3 = {h^u_{veryup}}^{-1}(w_3) = \left(u\left(k\right) + \frac{\Delta u}{2}\right) + w_3 \frac{\Delta u}{2} \tag{34}$$
$$u_4 = {h^u_{upcoming}}^{-1}(w_4) = u(k) + w_4 \Delta u \tag{35}$$
$$u_5 = {h^u_{previous}}^{-1}(w_5) = u(k) - (w_5 - 1)\,\Delta u \tag{36}$$
$$u_6 = {h^u_{verypre}}^{-1}(w_6) = u(k) - (w_6 - 1)\,\frac{\Delta u}{2} \tag{37}$$

(Case 2): $u(k+1) < u(k)$

$$u_1 = {h^u_{upcoming}}^{-1}(w_1) = u(k+1) - (w_1 - 1)\,\Delta u \tag{38}$$
$$u_2 = {h^u_{previous}}^{-1}(w_2) = u(k+1) + w_2 \Delta u \tag{39}$$
$$u_3 = {h^u_{veryup}}^{-1}(w_3) = u(k+1) - (w_3 - 1)\,\frac{\Delta u}{2} \tag{40}$$
$$u_4 = {h^u_{upcoming}}^{-1}(w_4) = u(k+1) - (w_4 - 1)\,\Delta u \tag{41}$$
$$u_5 = {h^u_{previous}}^{-1}(w_5) = u(k+1) + w_5 \Delta u \tag{42}$$
$$u_6 = {h^u_{verypre}}^{-1}(w_6) = \left(u\left(k+1\right) + \frac{\Delta u}{2}\right) + w_6 \frac{\Delta u}{2} \tag{43}$$

Finally, the inference result $u_{Fuzzy}(t)$ to fully encompass the six rules is provided by

$$u_{Fuzzy}(t) = \frac{\sum_{i=1}^{6} w_i u_i}{\sum_{i=1}^{6} w_i} \tag{44}$$

In Fig. 5, $u_{Fuzzy}(t)$ represents the control input instruction from the active powertrain vibration damping system inside time-zone (T3) $k\Delta T_{cont} < t < (k+1)\Delta T_{cont}$.

The proposed fuzzy rules: (Rules 1-6) in (10)-(15) are summarized in Table 2. The element where rules and fuzzy sets are not defined is denoted as the symbol "–".

TABLE 2. Rule table of fuzzy rules 1-6 (output: $u(t^*)$, input: t^* and $|\dot{y}_p|$).

		$\lvert\dot{y}_p\rvert \geq 0$		
		–	"Big"	"Small"
t^*	"Nearly upcoming step (ΔT_{cont})"	"Similar to $u(k+1)$"	–	–
	"Nearly previous step (0)"	"Similar to $u(k)$"	–	–
	"Nearly intermediate step ($\frac{1}{2}\Delta T_{cont}$) after it"	–	"Very similar to $u(k+1)$"	"Similar to $u(k+1)$"
	"Nearly intermediate step ($\frac{1}{2}\Delta T_{cont}$) before it"	–	"Similar to $u(k)$"	"Very similar to $u(k)$"

V. SIMULATION VALIDATIONS

A. SIMULATION SETTINGS

Simulation studies are carried out to verify the robustness of the fuzzy system. The objective in the simulations is to obtain a target response signal (smooth step) by the control objective, which is to dampen the X_B vehicle oscillation. At 2.0 s, there is a smooth change in the target response that does not involve vibrations from a negative value to a positive one. It is inspired by the circumstance which causes a sudden change in the driving force in actual automobiles. The transitional vibrations occurring in the vehicle body can be clearly assessed in this condition.

Table 3 shows the parameters for simulation setting. Fig. 7(a) shows the configuration of the Simulink environment used for the validations. The validations test the two cases: (Case 3) and (Case 4) on time-fluctuated control cycles like those indicated in Fig. 7(b).

TABLE 3. Parameters for simulation setting.

Properties	Value
ΔT_{cont}	0.0438 s
$\Delta T_{predict}$	2.0×10^{-5} s
$\lvert \dot{y}_p \rvert_{max}$	0.6 m/s
Sampling time	2.0×10^{-5} s
Plant parameter fluctuation	± 10 %

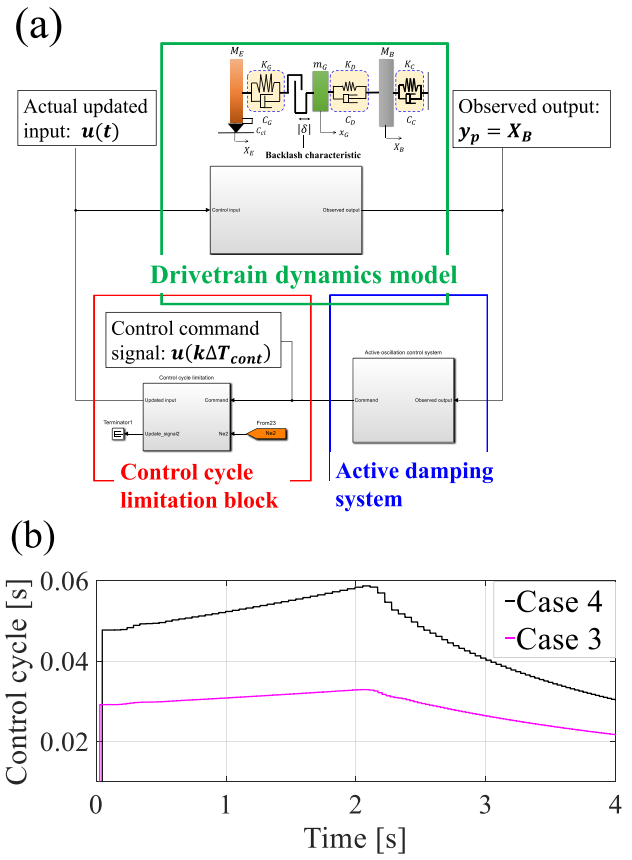

FIGURE 7. Simulation environment: (a) Simulink diagram and (b) two cases of the control period constraint.

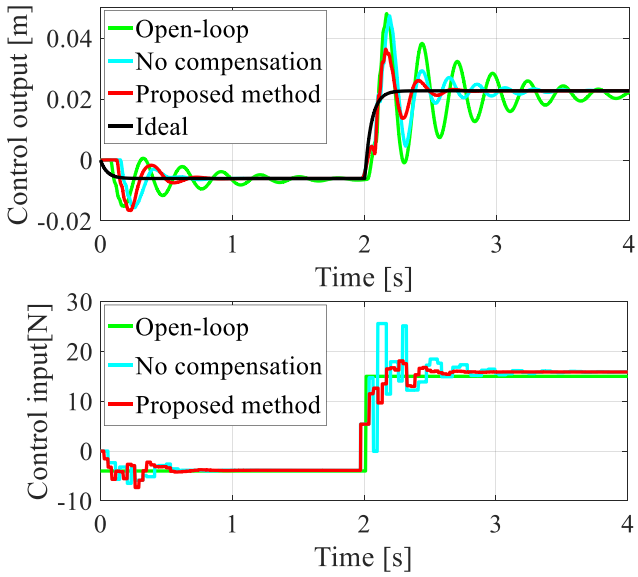

FIGURE 8. Time responses of the control input and vehicle vibration of the simulation (Case 3).

B. SIMULATION RESULTS AND DISCUSSION

The time responses of the vehicle vibration in the top graph and the control inputs in the lower graph are shown in Fig. 8 as the simulation result (Case 3).

The remaining vibration shown by the cyan line argues that only the traditional SDC with no compensations for the time-fluctuating control cycle is insufficient even though its transient characteristic is improved compared to the open-loop response (i.e., no controls) shown by the green line. On the other hand, the red line indicates that the vibration is considerably suppressed, meaning the contribution of the proposed fuzzy compensation to the improved response. Taking care of time-fluctuations in the update timings of the control input is crucial to bringing the response closer to the ideal one in the black line.

Another validation result (Case 4) is shown in Fig. 9. It can be observed that the vibration is deteriorated depending on cases of the time-fluctuated control cycle, as shown in the cyan line. Nevertheless, the proposed method (red line) consistently demonstrates the higher damping performance. This result proves the robustness to more patterns of the fluctuations in the control periods.

Regarding the result of Fig. 9, the time histories of the degree of match w_i $(0 \leq w_i \leq 1,\ i = 1, 2, \ldots 6)$ for Rules 1–6 at the update timing are summarized in Fig. 10. These results provide analysis material to discuss how much each rule was used. The remarkable point is that there are no unnecessary fuzzy rules. This can be found from the fact that all the rules take some values within the total simulation time. Even though Rules 1 and 2, which have the high values

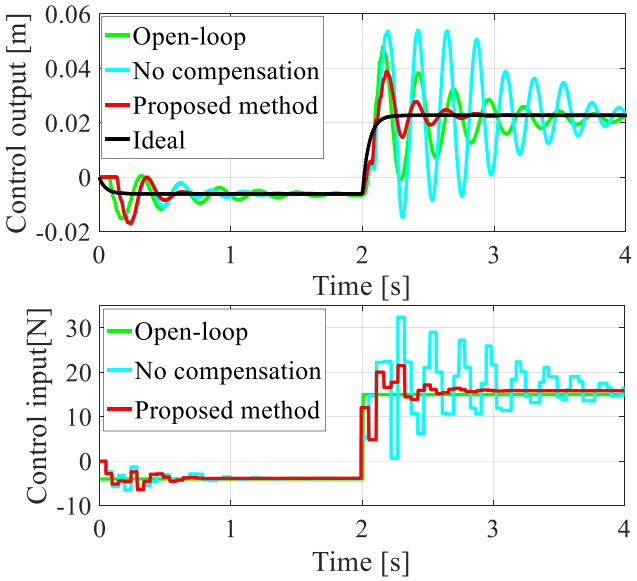

FIGURE 9. Time responses of the control input and vehicle vibration of the simulation (Case 4).

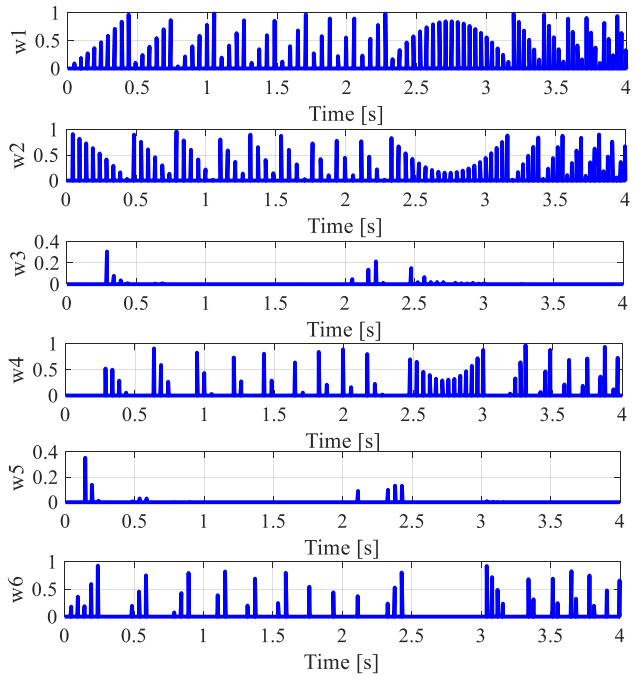

FIGURE 10. Degree of match w_i ($0 \leq w_i \leq 1, i = 1, 2, \ldots 6$) for Rules 1–6 at the update timing in the result of (Case 4).

of w_1 and w_2, are dominant over the other rules, we can see that Rules 3-6 are also frequently used after 2.0 seconds when active damping is especially required. Combined with discussion about Fig. 10, the result of Fig. 9 implies that a blend of all the rules contributes to improving the transient vehicle response.

In this study, we chose to observe the 2-norm of the vehicle body vibration response as the criteria used to evaluate the effectiveness of the control scheme. The 2-norm is well-known to be suitable for evaluating transient characteristics of a time response [27]. A smaller value of the 2-norm means better control performance (i.e., less oscillation) with a controller. Specifically, the 2-norm of this study is computed using the error between each controlled response and the ideal response as:

$$\|e\|_2 = \sqrt{\sum_{m=1}^{N} |e[m]|^2} = \sqrt{\sum_{m=1}^{N} |y[m] - r[m]|^2} \qquad (45)$$

The error, controlled response, ideal response at the mth sampling point are denoted as $e[m]$, $y[m]$, $r[m]$, respectively. N indicates the total number of sampling points.

Table 4 performs the quantitative comparison of each result in Figs. 8 and 9. Table 4 shows the smallest norm is achieved by the proposed fuzzy compensation. This means that the response by the proposed method is the closest to the ideal one.

TABLE 4. Quantitative performance index by 2-norm of each error between the vehicle vibration and the ideal response in simulation.

Each simulation result	2-norm in Fig. 8	2-norm in Fig.9
Open-loop	2.8499	2.8293
No compensation	1.9615	5.0432
Proposed method	1.3608	1.4803

C. COMPARISON WITH PREVIOUS APPROACH FOR ROBUSTNESS

Robustness tests are carried out to further confirm the effectiveness of the proposed approach. For Table 1, each drivetrain parameter is changed in relation to its nominal value. Table 5 shows the variation amount given for the parameters [28].

TABLE 5. Parameter variation given for the drivetrain.

Parameter	Variation amount [%]
M_B [kg]	10
m_G [kg]	−10
M_E [kg]	−10
K_C [N/m]	10
K_D [N/m]	10
K_G [N/m]	−10
C_C [Ns/m]	−10
C_D [Ns/m]	10
C_G [Ns/m]	−10
C_{cl} [Ns/m]	10

In addition, another control strategy, which is based on the elementary fuzzy inference compensation with only two output variables [27], [28] is tested just for comparison with the proposed method. The capability to deal with time-fluctuated control periods has been confirmed in the previous studies [27], [28].

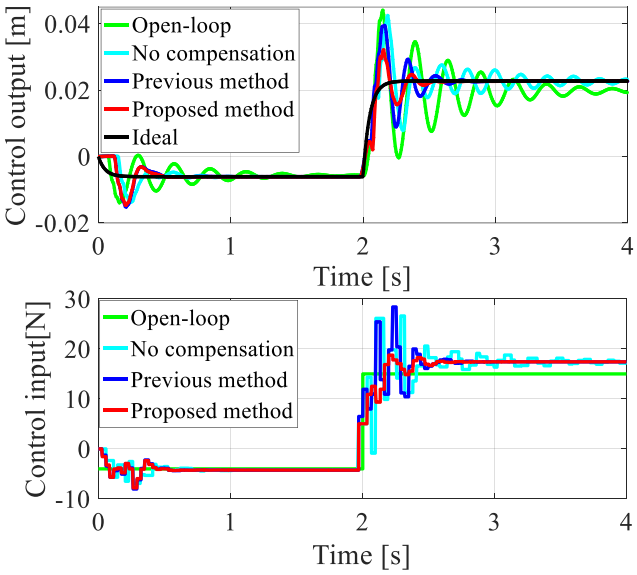

FIGURE 11. Comparison with the previous method under time-fluctuated control cycle, which is like (Case 3).

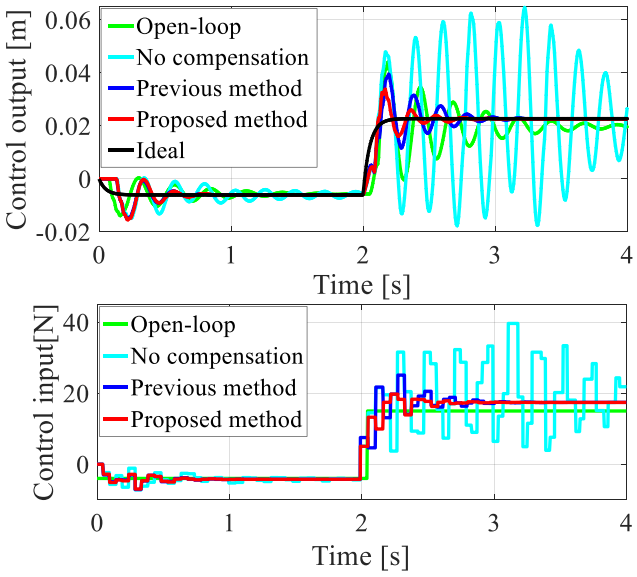

FIGURE 12. Comparison with the previous method under time-fluctuated control cycle, which is like (Case 4).

Figs. 11 and 12 show the test results under two patterns of the time-fluctuated control cycles, which are like (Case 3) and (Case4), respectively. As shown by the red and blue lines, both the proposed and previous fuzzy compensations improve the vibrations over the case with no compensations. Observed in detail, however, we can see that the proposed six rules-based fuzzy compensation (red line) has the better transient response than that by the previous fuzzy one (blue line). These results imply that there is a possibility that the six rules-based inference has a superiority over the previous one in terms of robustness.

The cause of such improvement is considered to be presence of the abundant linguistic expressions of the output variables defined in the six fuzzy rules. In the previous fuzzy compensation [27], [28], the flexibility in inference is insufficient due to few candidates of the control commands because it has only two output variables. To ensure the robustness, i.e., adaptability, to various conditions induced by severe fluctuations in the plant parameters and control cycles, it is necessary to prepare more options of the control commands. Such flexible inference is based on a rich diversity of output variables in the fuzzy rules. Therefore, the abundant linguistic expressions of the output variables: "similar to $u(k+1)$", "similar to $u(k)$", "very similar to $u(k+1)$", and "very similar to $u(k)$ can contribute to the robust performance shown in Figs. 11 and 12.

Table 6 performs the quantitative comparison of each result in Figs. 11 and 12. Table 6 shows that the smallest norm, which means the best vibration control performance, is achieved by the proposed fuzzy compensation.

TABLE 6. Quantitative performance index by 2-norm of each error between the vehicle vibration and the ideal response in simulation with robustness test.

Each simulation result	2-norm in Fig. 11	2-norm in Fig.12
Open-loop	2.5496	2.7049
No compensation	1.6088	7.1333
Previous method [28]	1.4416	1.5483
Proposed method	1.0329	1.2380

VI. EXPERIMENTAL VERIFICATIONS

A. RESULTS OF THE EXPERIMENT AND DISCUSSION

Finally, the system shown in Figs. 2 and 3 is used to experimentally verify the effectiveness of the vibration control strategy.

The test result, which is based on the control period limitation like (Case 1) shown in Fig. 3(b), is displayed in Fig. 13. Each color line corresponds to the same meaning as that in the simulation results.

Fig. 13 shows that the proposed method sufficiently suppresses the transient vibration after 2.0 s, realizing the almost ideal response. We can observe the need for compensating for variations in the control input update timings as well as the advantages of the fuzzy technique by comparing the proposed method's response to that given by "No compensation", which fails to reduce the vibration.

Here, the practical implications of the proposed technique need to be discussed. To implement control systems on real-world vehicles, it is necessary to reduce the computational loads so that the operation of a controller can be finished within a control period. Compared to the existing method (e.g., MPC), the proposed fuzzy strategy is more suitable for the implementation in that online iterative optimizations with heavy computational loads are unnecessary. In addition,

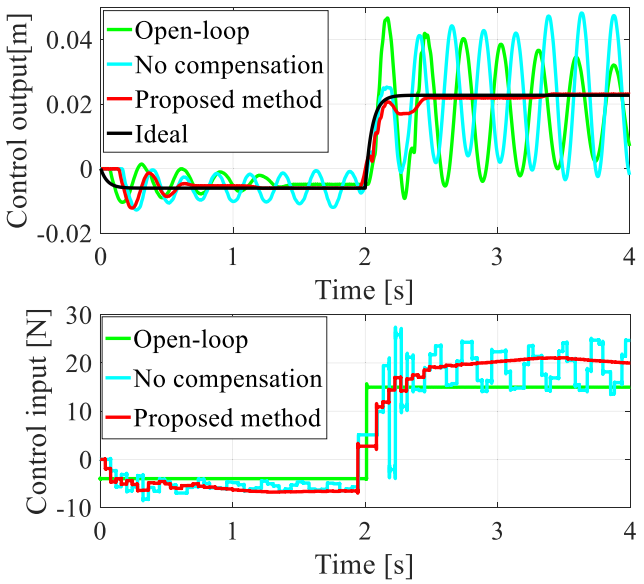

FIGURE 13. Experimental result under the time-fluctuated control cycle like (Case 1).

this approach is built upon the compensation mechanism emulating human intuition with abundant linguistic variables. This characteristic makes handling of the controller easier and eliminates the need for intricate modeling of control input update timings.

To observe the result of Fig. 13 in more details, Fig. 14 presents the enlarged view of the control input signals computed in the proposed active control system. The blue and cyan lines indicate $u(k)$ by the SDC and $u(k+1)$ by the model prediction, respectively. The black line indicates the control command by the fuzzy logic. The control input actually updated by the actuator is shown in the red line.

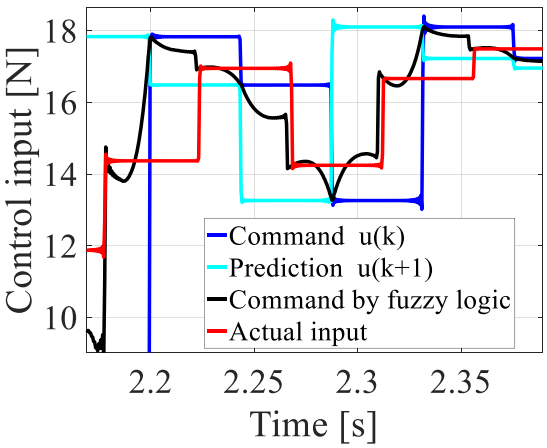

FIGURE 14. Enlarged view of the control input obtained by the fuzzy logic compensation.

We can see that $u(k)$ calculated by the SDC matches the predicted value $u(k+1)$ with a one-step delay. This means that online prediction of the plant dynamics is successfully achieved with the good accuracy. Such a well-performed model predictive technique is required for performing the fuzzy inference. In addition, Fig. 14 demonstrates that the control command by the fuzzy logic gradually changes between $u(k)$ and $u(k+1)$. This movement is due to employing the update timing t^* as the input variable to the fuzzy system. That is, the command indicated by the black line is determined by compromise of both signals $u(k)$ and $u(k+1)$.

Table 7 performs the quantitative comparison of each result in Fig. 13 via the 2-norm of the response. The smallest norm is obtained by the proposed method. Compared to "Open-loop" and "No compensation", the proposed method reduces the 2-norm by 80.2367% and 80.4455%, respectively, in Fig. 13. Consequently, the effectiveness of the proposed fuzzy system is quantitatively confirmed by the comparison experiment.

TABLE 7. Quantitative performance comparison by 2-norm in experiment.

Each experimental result	2-norm in Fig. 13
Open-loop	0.9875
No compensation	0.9980
Proposed method	0.1952

B. COMPARISON STUDY AND QUANTITATIVE PERFORMANCE ANALYSIS

Fig. 15 displays the comparison outcome between the proposed approach and another earlier strategy under the fluctuated control period like (Case 2). The latter one is the model-prediction-based compensation with SDC, which has been studied in the previous literature [23]. Fuzzy logic is not involved with this approach.

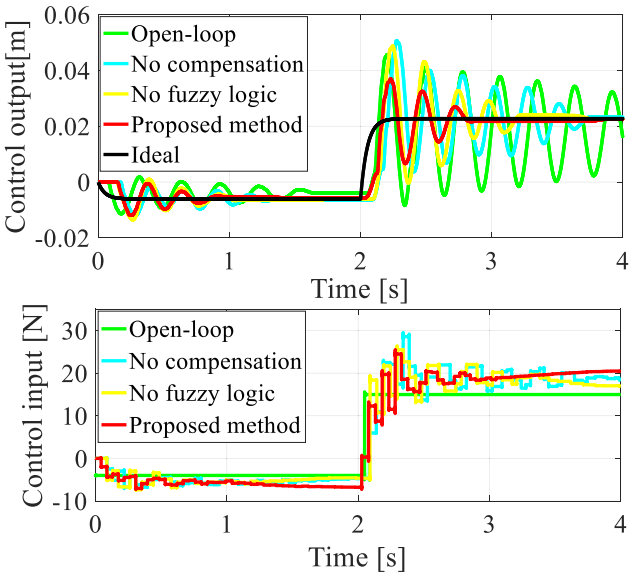

FIGURE 15. Experimental result under the time-fluctuated control cycle like (Case 2).

In Fig. 15, the best damping performance is given by the proposed method, as indicated by the comparison between each response. The larger vibration remains in the response (yellow line) by the model-prediction with no fuzzy inferences. This is because the previous strategy does not explicitly handle various fluctuated timings of updating the control input, even though only the maximal delay of it can be addressed. Against the previous system's drawback, the improvement indicated by the red line proves the efficacy of the application of fuzzy logic.

In Table 8, the above experimental result of Fig. 15 is quantitatively summarized in the form of 2-norm on each response. The performance analysis reveals that the proposed fuzzy-logic-based strategy offers higher vibration reduction levels despite fluctuations in the control period. Compared to ''Open-loop'', ''No compensation'' and ''No fuzzy logic'', the proposed method reduces the 2-norm by 56.5394%, 40.7869%, and 35.1716%, respectively, in Fig. 15.

TABLE 8. Quantitative performance comparison by 2-norm in comparative experiment with previous method.

Each experimental result	2-norm in Fig. 15
Open-loop	0.9768
No compensation	0.7169
No fuzzy logic [23]	0.6548
Proposed method	0.4245

Some limitations on this research should be described. Specifically, the control system contains design parameters that need to be tuned manually, sometimes hindering the smooth process of the implementation on real vehicles. Additionally, it is necessary to investigate the robustness of the fuzzy logic for a variety of driving situations and more severe fluctuations in the parameters. Nevertheless, they have not been yet carried out for real vehicles. Therefore, the introduction of optimization algorithms into powertrain controllers like those in the literatures [38], [39] and the verification using an actual test vehicle will be our future tasks.

VII. CONCLUSION

The contribution of this study is to develop a straightforward fuzzy compensation composed of six inference rules to tackle the problem of a time-varying control period constraint, which arises in the active vibration control of a drivetrain. The key finding is that changing update timings of the control input can be successfully managed by the fuzzy rules in the proposed system. This is based on the unique technique that represents the update timings as fuzzy sets with abundant linguistic expressions. The significant feature of the proposed six fuzzy rules is that it achieves the simple compensating mechanism inspired by human intuition, thereby eliminating the need for intricate and detailed modeling of control input update timings. The efficacy of the active damping technique was demonstrated through simulations and experiments using the abstract drivetrain mechanism. The verifications presented the significant finding: the robustness of the proposed approach in dealing with substantial changes in the control period, when compared to previous control strategies.

In the future, the proposed approach will be implemented in real-world vehicles to investigate the practicability and robustness. In addition, our future works include the introduction of optimization algorithms to eliminate the need for manual tunings of the controller parameters.

REFERENCES

[1] C. Ahumada and P. Wheeler, ''Reduction of torsional vibrations excited by electromechanical interactions in more electric systems,'' *IEEE Access*, vol. 9, pp. 95036–95045, 2021, doi: 10.1109/ACCESS.2021.3094172.

[2] A. G. A. Muthalif, K. A. M. Nor, A. N. Wahid, and A. Ali, ''Optimization of piezoelectric sensor-actuator for plate vibration control using evolutionary computation: Modeling, simulation and experimentation,'' *IEEE Access*, vol. 9, pp. 100725–100734, 2021, doi: 10.1109/ACCESS.2021.3096972.

[3] Z. Hao, T. Wang, X. Cao, and Q. Zhang, ''Design of eccentric mass-type vibration-damping electric actuator control system for non-fixed-wing aircraft,'' *IEEE Access*, vol. 8, pp. 219415–219429, 2020, doi: 10.1109/ACCESS.2020.3042854.

[4] E. Atam, ''Friction damper-based passive vibration control assessment for seismically-excited buildings through comparison with active control: A case study,'' *IEEE Access*, vol. 7, pp. 4664–4675, 2019, doi: 10.1109/ACCESS.2018.2886880.

[5] A. Yonezawa, I. Kajiwara, and H. Yonezawa, ''Novel sliding mode vibration controller with simple model-free design and compensation for actuator's uncertainty,'' *IEEE Access*, vol. 9, pp. 4351–4363, 2021, doi: 10.1109/ACCESS.2020.3047810.

[6] Z. Jinyu, H. Song, J. Longyu, and Y. Fuyuan, ''Active vibration control strategy for online application in a range extender,'' *IEEE Access*, vol. 11, pp. 26686–26702, 2023, doi: 10.1109/ACCESS.2023.3255418.

[7] C. Lv, J. Zhang, Y. Li, and Y. Yuan, ''Mode-switching-based active control of a powertrain system with non-linear backlash and flexibility for an electric vehicle during regenerative deceleration,'' *Proc. Inst. Mech. Eng., D, J. Automobile Eng.*, vol. 229, no. 11, pp. 1429–1442, Sep. 2015, doi: 10.1177/0954407014563552.

[8] Z. Zhou, R. Guo, and X. Liu, ''A disturbance-compensation-based sliding mode control scheme on mode switching condition for hybrid electric vehicles considering nonlinear backlash and stiffness,'' *J. Vib. Control*, vol. 29, nos. 15–16, pp. 3823–3837, May 2022, doi: 10.1177/10775463221096195.

[9] P. Templin and B. Egardt, ''A powertrain LQR-torque compensator with backlash handling,'' *Oil Gas Sci. Technol.-Revue d'IFP Energies nouvelles*, vol. 66, no. 4, pp. 645–654, Jul. 2011, doi: 10.2516/ogst/2011147.

[10] Y. Yue, Y. Huang, D. Hao, and G. G. Zhu, ''Model reference adaptive LQT control for anti-jerk utilizing tire-road interaction characteristics,'' *Proc. Inst. Mech. Eng., D, J. Automobile Eng.*, vol. 235, no. 6, pp. 1670–1684, May 2021, doi: 10.1177/0954407020973971.

[11] X. Lu, T. Lu, and B. Chai, ''Mode-switch model predictive controller with 'pre-contact' method for alleviating driveline vibration of electric vehicles considering backlash,'' *Proc. Inst. Mech. Eng., D: J. Automobile Eng.*, vol. 234, no. 8, pp. 2176–2194, Jul. 2020, doi: 10.1177/0954407019898363.

[12] O. Atabay, M. Ötkür, and İ. M. Ereke, ''Model based predictive engine torque control for improved drivability,'' *Proc. Inst. Mech. Eng., D, J. Automobile Eng.*, vol. 232, no. 12, pp. 1654–1666, Oct. 2018, doi: 10.1177/0954407017733867.

[13] X. Chen, D. Peng, J. Hu, C. Li, S. Zheng, and W. Zhang, ''Adaptive torsional vibration active control for hybrid electric powertrains during start-up based on model prediction,'' *Proc. Inst. Mech. Eng., D, J. Automobile Eng.*, vol. 236, nos. 10–11, pp. 2219–2229, Nov. 2021, doi: 10.1177/09544070211056176.

[14] A. Yüceşan and A. Mugan, ''Development of a model predictive controller for an active torsional vibration damper to suppress torsional vibrations in vehicle powertrains,'' *Proc. Inst. Mech. Eng., D, J. Automobile Eng.*, vol. 236, no. 1, pp. 127–141, Jan. 2022, doi: 10.1177/09544070211014791.

[15] S. Thiyagarajan, E. Varuvel, V. Karthickeyan, A. Sonthalia, G. Kumar, C. G. Saravanan, B. Dhinesh, and A. Pugazhendhi, "Effect of hydrogen on compression-ignition (CI) engine fueled with vegetable oil/biodiesel from various feedstocks: A review," *Int. J. Hydrogen Energy*, vol. 47, no. 88, pp. 37648–37667, Oct. 2022, doi: 10.1016/j.ijhydene.2021.12.147.

[16] H. T. Arat, "Alternative fuelled hybrid electric vehicle (AF-HEV) with hydrogen enriched internal combustion engine," *Int. J. Hydrogen Energy*, vol. 44, no. 34, pp. 19005–19016, Jul. 2019, doi: 10.1016/j.ijhydene.2018.12.219.

[17] H. T. Arat, "Simulation of diesel hybrid electric vehicle containing hydrogen enriched CI engine," *Int. J. Hydrogen Energy*, vol. 44, no. 20, pp. 10139–10146, Apr. 2019, doi: 10.1016/j.ijhydene.2018.10.004.

[18] M. Berriri, P. Chevrel, and D. Lefebvre, "Active damping of automotive powertrain oscillations by a partial torque compensator," *Control Eng. Pract.*, vol. 16, no. 7, pp. 874–883, Jul. 2008, doi: 10.1016/j.conengprac.2007.10.010.

[19] J. Baumann, D. D. Torkzadeh, A. Ramstein, U. Kiencke, and T. Schlegl, "Model-based predictive anti-jerk control," *Control Eng. Pract.*, vol. 14, no. 3, pp. 259–266, Mar. 2006, doi: 10.1016/j.conengprac.2005.03.026.

[20] M. Mattsson, R. Mehler, M. Jonasson, and A. Thomasson, "Optimal model predictive acceleration controller for a combustion engine and friction brake actuated vehicle," *IFAC-PapersOnLine*, vol. 49, no. 11, pp. 511–518, 2016, doi: 10.1016/j.ifacol.2016.08.075.

[21] R. S. Vadamalu and C. Beidl, "Adaptive internal model-based harmonic control for active torsional vibration reduction," *IEEE Trans. Ind. Electron.*, vol. 67, no. 4, pp. 3024–3032, Apr. 2020, doi: 10.1109/TIE.2019.2908579.

[22] Y. Huang, J. Wang, Y. Yue, and L. Yang, "Model predictive control for active vibration suppression of hybrid electric vehicles during mode transition," *Proc. Inst. Mech. Eng., D, J. Automobile Eng.*, vol. 237, no. 12, pp. 2819–2830, Aug. 2022, doi: 10.1177/09544070221117336.

[23] H. Yonezawa, I. Kajiwara, C. Nishidome, T. Hatano, M. Sakata, and S. Hiramatsu, "Active vibration control of automobile drivetrain with backlash considering time-varying long control period," *Proc. Inst. Mech. Eng., D, J. Automobile Eng.*, vol. 235, nos. 2–3, pp. 773–783, Feb. 2021, doi: 10.1177/0954407020949428.

[24] N. Khan, D. A. Elizondo, L. Deka, and M. A. Molina-Cabello, "Fuzzy logic applied to system monitors," *IEEE Access*, vol. 9, pp. 56523–56538, 2021, doi: 10.1109/ACCESS.2021.3072239.

[25] M. Rabah, H. Haghbayan, E. Immonen, and J. Plosila, "An Ai-in-loop fuzzy-control technique for UAV's stabilization and landing," *IEEE Access*, vol. 10, pp. 101109–101123, 2022, doi: 10.1109/ACCESS.2022.3208685.

[26] M. Ahmadi Kamarposhti, H. Shokouhandeh, M. Alipur, I. Colak, H. Zare, and K. Eguchi, "Optimal designing of fuzzy-PID controller in the load-frequency control loop of hydro-thermal power system connected to wind farm by HVDC lines," *IEEE Access*, vol. 10, pp. 63812–63822, 2022, doi: 10.1109/ACCESS.2022.3183155.

[27] H. Yonezawa, A. Yonezawa, T. Hatano, S. Hiramatsu, C. Nishidome, and I. Kajiwara, "Experimental verification of active damping of powertrain vibrations with simple fuzzy logic compensation for time-varying control period," *Proc. Inst. Mech. Eng., D, J. Automobile Eng.*, Jun. 2023, Art. no. 095440702311781, doi: 10.1177/09544070231178103.

[28] H. Yonezawa, A. Yonezawa, T. Hatano, S. Hiramatsu, C. Nishidome, and I. Kajiwara, "Fuzzy-reasoning-based robust vibration controller for drivetrain mechanism with various control input updating timings," *Mechanism Mach. Theory*, vol. 175, Sep. 2022, Art. no. 104957, doi: 10.1016/j.mechmachtheory.2022.104957.

[29] H. Yonezawa, I. Kajiwara, S. Sato, C. Nishidome, M. Sakata, T. Hatano, and S. Hiramatsu, "Vibration control of automotive drive system with nonlinear gear backlash," *J. Dyn. Syst., Meas., Control*, vol. 141, no. 12, pp. 1–11, Dec. 2019, Art. no. 121002, doi: 10.1115/1.4044614.

[30] H. Yonezawa, I. Kajiwara, C. Nishidome, S. Hiramatsu, M. Sakata, and T. Hatano, "Vibration control of automotive drive system with backlash considering control period constraint," *J. Adv. Mech. Des., Syst., Manuf.*, vol. 13, no. 1, 2019, Art. no. JAMDSM0018, doi: 10.1299/jamdsm.2019jamdsm0018.

[31] H. Yonezawa, I. Kajiwara, S. Sato, C. Nishidome, T. Hatano, and S. Hiramatsu, "Application of physical function model to state estimations of nonlinear mechanical systems," *IEEE Access*, vol. 9, pp. 12002–12018, 2021, doi: 10.1109/ACCESS.2021.3051421.

[32] J. C. Gerdes and V. Kumar, "An impact model of mechanical backlash for control system analysis," in *Proc. Amer. Control Conf.*, pp. 3311–3315, doi: 10.1109/ACC.1995.532216.

[33] M. Nordin, J. Galic, and P.-O. Gutman, "New models for backlash and gear play," *Int. J. Adapt. Control Signal Process.*, vol. 11, no. 1, pp. 49–63, 1997.

[34] B. Bamieh and J. B. Pearson, "The H_2 problem for sampled-data systems," *Syst. Control Lett.*, vol. 19, no. 1, pp. 1–12, Jul. 1992, doi: 10.1016/0167-6911(92)90033-O.

[35] P. P. Khargonekar and N. Sivashankar, "H_2 optimal control for sampled-data systems," *Syst. Control Lett.*, vol. 17, no. 6, pp. 425–436, Dec. 1991, doi: 10.1016/0167-6911(91)90082-P.

[36] P. K. Gupta and P. K. Muhuri, "Extended Tsukamoto's inference method for solving multi-objective linguistic optimization problems," *Fuzzy Sets Syst.*, vol. 377, pp. 102–124, Dec. 2019, doi: 10.1016/j.fss.2019.02.022.

[37] S. Diana and A. Nugroho, "Mobile expert system using fuzzy Tsukamoto for diagnosing cattle disease," *Proc. Comput. Sci.*, vol. 116, pp. 27–36, Jan. 2017, doi: 10.1016/j.procs.2017.10.005.

[38] J. J. Eckert, T. P. Barbosa, F. L. Silva, V. R. Roso, L. C. A. Silva, and L. A. R. da Silva, "Optimum fuzzy logic controller applied to a hybrid hydraulic vehicle to minimize fuel consumption and emissions," *Expert Syst. Appl.*, vol. 207, Nov. 2022, Art. no. 117903, doi: 10.1016/j.eswa.2022.117903.

[39] J. J. Eckert, S. F. da Silva, F. M. Santiciolli, Á. C. de Carvalho, and F. G. Dedini, "Multi-speed gearbox design and shifting control optimization to minimize fuel consumption, exhaust emissions and drivetrain mechanical losses," *Mechanism Mach. Theory*, vol. 169, Mar. 2022, Art. no. 104644, doi: 10.1016/j.mechmachtheory.2021.104644.

HEISEI YONEZAWA (Member, IEEE) received the B.S., M.S., and Ph.D. degrees in engineering from Hokkaido University, Japan, in 2017, 2019, and 2021, respectively. Since 2021, he has been an Assistant Professor with the Graduate School of Engineering, Hokkaido University. His research interests include powertrain, vehicle systems, vibration control, robust control, and optimization. He received the Miura Prize for best students in the field of mechanical engineering from the Japan Society of Mechanical Engineers, in 2019.

ANSEI YONEZAWA (Member, IEEE) received the B.S., M.S., and Ph.D. degrees in engineering from Hokkaido University, Japan, in 2019, 2021, and 2023, respectively. Since 2023, he has been a Specially Appointed Assistant Professor with the Graduate School of Engineering, Hokkaido University. His research interests include active vibration control, robust control, stochastic optimization, fractional-order control, and data-driven control. He received the Hatakeyama Prize and the Miura Prize given for best students in the field of mechanical engineering from the Japan Society of Mechanical Engineers, in 2019 and 2021, respectively.

ITSURO KAJIWARA received the B.S. degree in engineering from Tokyo Metropolitan University, in 1986, and the M.S. and Ph.D. degrees in engineering from the Tokyo Institute of Technology, in 1988 and 1993, respectively. From 1990 to 2000, he was an Assistant Professor with the School of Engineering, Tokyo Institute of Technology. From 2000 to 2008, he was an Associate Professor with the Graduate School of Engineering, Tokyo Institute of Technology. Since 2009, he has been a Professor with the Graduate School of Engineering, Hokkaido University. His research interests include vibration, control, structural health monitoring, and laser application.